DEPARTMENT OF TRANSPORTATION

COAST GUARD

A TWO DIMENSIONAL MODEL

OF

WIND FORCED

INERTIAL OSCILLATIONS

Oceanographic Unit Technical Report 82-3
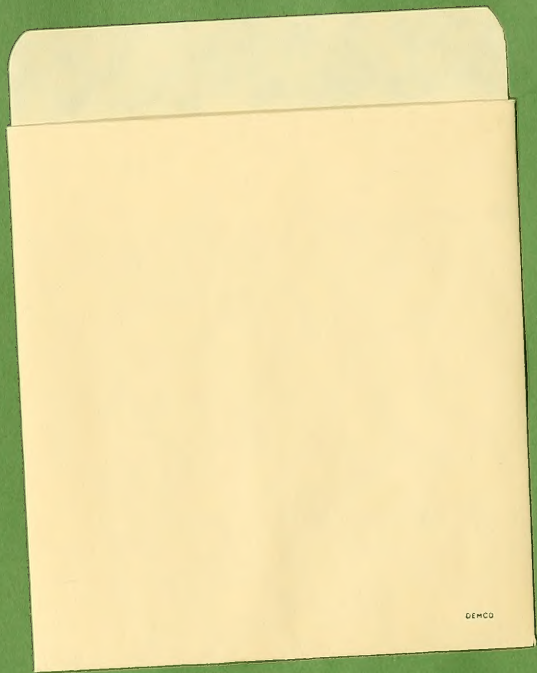
DEMCO

ABSTRACT

A two dimensional model of wind driven inertial oscillations is formulated. The equations for current velocity model the wind stress as a body force, and are vertically integrated in accordance with the "slab flow" concept. Two dissipation terms are included, one first order and a second order term. A linear constant of proportionality is used for each.

The changing nature of the thermocline is modeled using the equations of Denman (1973). A general algorithm is used for the solar radiative flux.

A numerical solution is developed for the system of equations. The portion of the model dealing with thermocline changes is tested against data from Ocean Station Papa. A good fit is obtained, with coefficients similar to those found by Denman and Miyake (1973).

Current velocities were tested against moored data using progressive vector diagrams. A good fit is obtained. The four day damping of Pollard and Millard (1970) is supported.

An experimental design is proposed to obtain two dimensional data for the testing of this type of model.
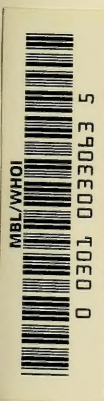
A TWO DIMENSIONAL MODEL OF WIND FORCED INERTIAL OSCILLATIONS

BRUCE E. VIEKMAN

INTRODUCTION

Recently several papers have investigated inertial oscillations in the mixed layer. Pollard (1970) showed that, for times less than seasonal, the wind stress at the surface is confined to the layer bounded below by the thermocline, and that the wind stress can be applied as a body force in that layer. Pollard and Millard (1970) used Pollard's development and a linear damping term to successfully model inertial oscillations in the North Atlantic 130 miles south of Nantucket.

Other papers have investigated the deepening of the mixed layer. Pollard, Rhines and Thompson (1973) investigated the deepening of the mixed layer for times up to inertial, using the temperature gradient below the mixed layer to quantify the stability of the fluid below the layer and entrainment rate of that fluid to deepen the wind forced layer. Niiler (1977) modeled the behavior of the mixed layer on a seasonal time scale. Denman (1973) used a mechanism similar to that used by Pollard, Rhines and Thompson to determine the deepening of the mixed layer using solar radiation and wind stress as forcing functions. Denman and Miyake (1973) used Denman's formulation to successfully model behavior of the thermocline at Ocean Station Papa (50°N, 145°W).

My objective is to combine these two separate trains of research and formulate an integrated, two dimensional model of mixed layer behavior for times of up to two weeks. This integration is important because the changing nature of the thermocline affects directly the currents in it, as we shall later find. To my knowledge, this is the first attempt to combine these two lines of investigation.

My motivation in pursuing this research was two-fold. First was the pure science of the sub- ject, and second was to fill a gap in the Coast Guard's Search and Rescue problem. The determination of the wind current as part of a prediction of the location of an object in the water has long been a problem to SAR planners, and I hope to give a more scientific aspect to this prediction. This goal of formulating an operational model imposed several constraints on its development which I will discuss throughout this paper.

THE MODEL

The formulation of the model is divided into two sections. One concerns the currents in the mixed layer, the second concerns the changes in the thermal structure of the upper ocean.

1. *Inertial Oscillations in the Mixed Layer.*

The mixed layer is assumed to be incompressible, in hydrostatic equilibrium, with a Rossby number less than one. It obeys the Boussinesq approximation. Vertical mean velocities are assumed to be zero. The mixed layer is bounded above by the sea surface and below by a density gradient. The ocean is assumed to be laterally unbounded and horizontally homogeneous. The wind stress is assumed to be zonal. The entire mixed layer is assumed to be highly turbulent and homogeneous. The distribution of all stresses and the diffusion of all properties in the layer are rapid, because of the highly turbulent nature of the layer.

The assumption that the mixed layer is bounded by a density gradient is based on the work of Pollard (1970). He showed that only a small part of the wind energy penetrates below the buoyancy frequency gradient, for times under my consideration. Here the thermocline is considered to be synonymous with the buoyancy frequency and density gradients under discussion.

1

With these assumptions, the equations of motion are reduced to:

$$\frac{\partial u}{\partial t} = fv - \frac{\partial}{\partial x}\overline{\rho u'u'} - \frac{\partial}{\partial y}\overline{\rho u'v'} - \frac{\partial}{\partial z}\overline{\rho u'w'} \tag{1.1}$$

$$\frac{\partial v}{\partial t} = -fu - \frac{\partial}{\partial x}\overline{\rho u'v'} - \frac{\partial}{\partial y}\overline{\rho v'v'} - \frac{\partial}{\partial z}\overline{\rho v'w'} \tag{1.2}$$

Equations 1.1 and 1.2 are then integrated from the sea surface to the mixed layer depth D, in accordance with the highly turbulent nature of the mixed layer.

The question of how much of a density gradient is enough to put a boundary on the mixed layer is a valid one. Because of the two dimensional nature of this model, and the inclusion of the changing thermocline structure, I hold that any gradient is enough to satisfy the definition. A large gradient will put a strong bound on the layer because of stratification. A small gradient will allow more of the wind stress to act on the fluid below the layer definition, and this action will be seen as a deepening of the thermocline. For the case of initially small stratification, deepening will occur until an equilibrium condition is met, as we shall see in the later sections of this report.

The mixed layer is conceptualized as sliding over the stable fluid below, since the density gradient at its lower interface provides for little turbulence at the base of the mixed layer. Thus the mixed layer acts as a slab of water moving in body. (Pollard and Millard, 1970; Denman and Miyake, 1973.)

The reason for this integration, and the subsequent abandonment of the Ekman (1905) development is for several reasons. First, I differ with Ekman's assumption of a vertically homogeneous fluid (constant A_z), since the mixed layer is bounded below by the thermocline, which places a limit on the downward penetration of wind energy.

Ekman dynamics could be considered for use in a development such as this if certain conditions were met, as a laminar flow situation, and little turbulent mixing (low A_z). Laminar flow is an implicit assumption in Ekman's development, since the only communication between "layers" in his equations are their boundary stresses. Laminar flow is a necessary condition for low turbulent mixing. I hold that the only way for Ekman dynamics to be used in this problem

would be if the depth of frictional resistance was to be less than the mixed layer depth in a low turbulence situation, since the thermocline prevents further downward penetration of wind energy (Pollard, 1970). At 45°N, the necessary A_z for a depth of frictional resistance of 45 meters, a reasonable estimate of most layer thicknesses, is 1.1×10^2 gm cm^{-1}sec^{-1}, which is one order of magnitude less than the usually accepted range for A_z of 10^3 to 10^7.

All of these preceding conditions listed as necessary for Ekman dynamics are violated by the turbulence in the mixed layer. The flow is not laminar, as the wind energy increases turbulence in the mixed layer. This wind induced turbulence increases the A_z which further deepens the theoretical mixed layer required for Ekman dynamics to be used. For a wind increase from 4 m sec^{-1} to 18 m sec^{-1}, the corresponding rise in A_z is from 58 gm cm^{-1} sec^{-1} to 2520 gm cm^{-1} sec^{-1} (Neumann and Pierson, 1966). Therefore, at a wind speed of 18 m sec^{-1}, the resulting depth of frictional resistance, and the required depth of the mixed layer for Ekman dynamics to exist, would be 219.66 meters. This is much deeper than the vast majority of observed mixed layer thicknesses.

The Reynolds stresses in the vertical are set equal to the overall vertical stress.

After integrating from the sea surface to D, assuming $\rho=1$, and dividing by D after the integration, equations 1.1 and 1.2 become

$$\frac{\partial u}{\partial t} = fv - \frac{\tau_{0x}}{D} - \frac{\tau_{Dx}}{D} - \frac{\partial}{\partial x}\overline{u'u'} - \frac{\partial}{\partial y}\overline{u'v'} \tag{1.3}$$

$$\frac{\partial v}{\partial t} = -fu - \frac{\tau_{0y}}{D} - \frac{\tau_{Dy}}{D} - \frac{\partial}{\partial x}\overline{u'v'} - \frac{\partial}{\partial y}\overline{v'v'} \tag{1.4}$$

where τ_{0x} is the stress at the sea surface in the x direction, τ_{0y} the surface stress in the y direction, and τ_{Dx}, τ_{Dy} is the stress on the bottom of the mixed layer over the stable fluid below. By the elimination of the internal vertical Reynolds stresses I hold that the only vertical stresses that can occur in the mixed layer are those caused by boundary processes.

Since predictions of the horizontal Reynolds stresses in the mixed layer cannot be made, and prediction of the amount of momentum transfer through the thermocline is extremely difficult, the equations will have to be altered if they are to be used in any but a "frictionless" form.

If we assume, as an aside, that the motion is frictionless, and the wind stress is limited to the +x direction, the equations can be easily solved analytically by taking the time derivative of the frictionless form of 1.4. Substituting in the friction-less form of 1.3 I obtain a linear second order partial differential equation, which is solved to be:

$$v = \frac{-\tau_o}{Df} \, (\text{I-cos ft}) \tag{1.5}$$

$$u = \frac{\tau_o}{Df} \, (\text{SIN ft}) \tag{1.6}$$

These equations describe an oscillatory flow 90 degrees cum sole to the wind, in a "hopping" motion. Each "hop" takes one inertial period, and will persist into infinity as long as the wind stress is constant (Kollmeyer, 1978).

The form of the Reynolds stress terms imply a dependence on velocity squared for the amount of turbulent dissipation of energy within the fluid. A proportionality factor, assumed to be linear, is also necessary. To make the equations stable in a computer time stepped format, the following form was used:

$$-\left(\frac{\partial}{\partial x} \, \overline{u'u'} + \frac{\partial}{\partial y} \, \overline{u'v'}\right) = -K_1\sqrt{u^2+v^2}\,{}^1 u \tag{1.7}$$

$$-\left(\frac{\partial}{\partial x} \, \overline{u'v'} + \frac{\partial}{\partial y} \, \overline{v'v'}\right) = -K_2\sqrt{u^2+v^2}\,{}^1 v \tag{1.8}$$

The terms defining the drag on the bottom of the layer, τ_D, were quantified in a similar manner to the Reynolds stress terms. The D in the denominator was dropped because the drag at the bottom of the layer should be dependent on the stratification below the mixed layer, not on the depth of the layer itself. Since the current velocities in the mixed layer are a function of its depth, any effects of the depth of the layer on the dissipation function would be taken into account by the coefficient and the velocity on which it acts.

$$\frac{\tau_{DX}}{D} = K_2 u \tag{1.9}$$

$$\frac{\tau_{DY}}{D} = K_2 v \tag{1.10}$$

Substituting 1.7 through 1.10 into 1.3 and 1.4, we have final form of the motion equations.

$$\frac{\partial u}{\partial t} = fv + \frac{\tau_{OX}}{D} - K_1\sqrt{u^2+v^2}\,{}^1 u - K_2 u \tag{1.11}$$

$$\frac{\partial v}{\partial t} = -fu + \frac{\tau_{OY}}{D} - K_1\sqrt{u^2+v^2}\,{}^1 v - K_2 v \tag{1.12}$$

Several facets of these equations deserve mention. The wind stress is modeled as a body force over the entire mixed layer, as was shown to be valid by Pollard (1970). The equations obey the concept of "slab flow", as have most models developed recently.

The formulation of the dissipation functions is designed to take into account first and second order dissipations that could be acting on the mixed layer. The terms are designed to span the large gap in the current knowledge of regarding downward momentum transport and turbulent energy dissipation. In testing the model, the K_1 and K_2 coefficients will be adjusted to fit the data base.

Another aspect of the equations is the shifting of the dominant frequency of the model to somewhat greater than f^{-1}, because of the subtraction of the dissipation terms (Pollard and Millard, 1970). This effect would be maximum during a period of steady, unidirectional winds. In testing the model, it was found that this effect was not significant enough to warrant an alteration to the coriolis parameter, as was contemplated to bring the model's dominant frequency into line with the natural inertial frequency at the latitude modeled.

The surface wind stress, τ_O, was determined using the Bodine (1971) formulation. His equations for the wind stress are:

$$\tau_O = \overline{u}_{10}^2 \, \times 1.1 \times 10^{-6} \tag{1.13}$$

for winds of less than 715 cm sec^{-1} and

$$\tau_O = \overline{u}_{10}^2 \, ((1-715/\overline{u}_{10})^2 \times 2.5 \times 10^{-6}) + 1.1 \times 10^{-6} \tag{1.14}$$

for winds greater than 715 cm sec^{-1}. Bodine's fomulation has a transition point at 14 knots, which takes into account the more turbulent nature of higher wind velocities and, to a more limited degree, the higher pressure differentials on the leeward and windward sides of surface waves at the higher wind velocities.

3

The calculated wind stress is applied directly to the mixed layer, since it has been shown (Richman and Garrett, 1977) that 97% of the momentum input to the surface is transmitted eventually to the mixed layer. If a more substantial portion of the wind energy had been advected away by surface waves, the wind stress into the mixed layer would have to be reduced by some factor.

Equations 1.11 through 1.14 were solved numerically at each time step, as analytical solutions are not possible.

2. Mixed Layer Deepening and Thermocline Changes.

An important construct in the motion equations is the mixed layer depth D. When the wind forces the mixed layer into motion, the magnitude of this forcing function is determined by both the magnitude of the wind stress and the depth of the mixed layer, because of the application of the wind stress as a body force.

It is important to include not only deepening of the layer due to unstable internal waves at the interface of the moving water and the stable fluid below (Pollard, Rhines and Thompson, 1973), but also the possibility of the formation of a shallow lens of warmer water near the surface due to low mixing by the wind and high solar radiation. This shallower layer of warm water would then become the layer acted on by the wind stress, because the density gradient caused by temperature at its base would then be the barrier to the penetration of the wind's energy.

Figure 2.1 illustrates this phenomenon. 2.1(a) is at the conclusion of some wind event, with a fully developed mixed layer. 2.1(b) is at some time later than (a). In the interim, there has been a period of relative calm, with solar heating, D_2, the new mixed layer depth is much less than D_1, the previous depth. At some new wind event, the controlling depth for the calculations would be D_2, because of the thermal gradient at $z=D_2$. At this new wind event, the old motions of the water below the new mixed layer depth D_2 would continue unforced because the wind energy would be limited in its penetration into the water by the temperature and density gradient at $z=D_2$. Velocity shears can therefore occur at the boundary between the new and old mixed layers, at depth D_2. These velocity shears may be responsible for observations in the deep oceans of structures interpreted as Ekman spirals (Assaf, Gerard and Gordon, 1971).
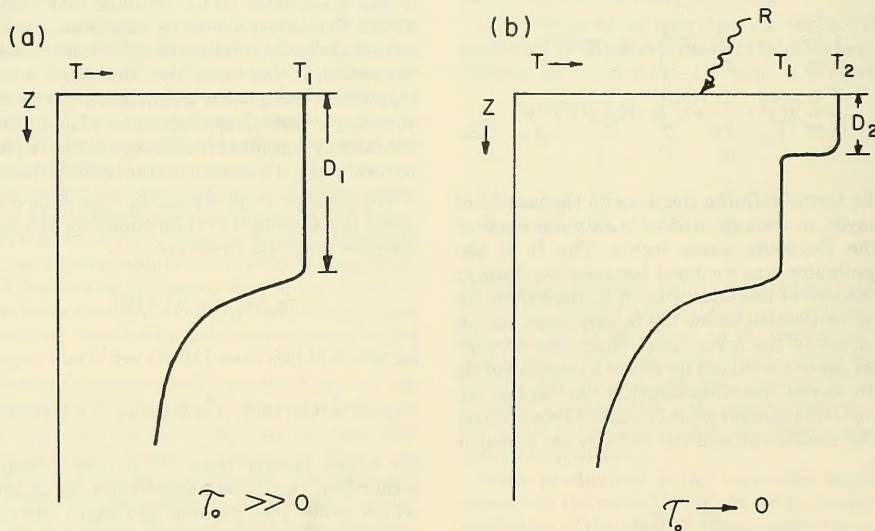

Figure 2.1 Schematic or the Formation of a New, Shallow Mixed Laver by Low Winds and Insolation.

Because of the importance of the possible shoaling of the mixed layer depth to a two dimensional model, I sought a formulation including this possibility.

After reviewing the literature, I decided to use the Denman (1973) formulation as applied by Denman and Miyake (1973), and some elements of the Pollard, Rhines and Thompson (1973) model.

I will outline the components of the Denman (1973) derivation for application. His assumptions are similar to mine, with the added assumption that all inputs to the mixed layer are redistributed uniformly by turbulent diffusion, and the time required for this distribution is small, assumed to be instantaneous. Denman also assumes that density is controlled only by temperature, as salinity is assumed to be constant throughout the mixed layer. In applying his derivation, I assume $w = 0$, because any mean upwelling velocities are small compared to the rate at which the mixed layer deepens.

Using the equations for conservation of thermal energy and conservation of mechanical energy, he derives four equations for the thermal behavior of the layer. Assuming H_e and H_s, the turbulent exchanges of heat at the sea surface equal to zero, gives:

$$\frac{\partial T_s}{\partial t} = \frac{2}{D^2} \ [-(G-D') + DB + R(D - \delta^{-1} + \delta^{-1}e^{-\delta D})] \tag{2.1}$$

$$H \ \frac{\partial D}{\partial t} = \frac{2[(G-D') + R\delta^{-1}(1-e^{-\delta D})] - D[B + R(1+e^{-\delta D})]}{D(T_s - T_{-D})} \tag{2.2}$$

$$\frac{\partial}{\partial t} \ T_{-D} = \delta Re^{-D} \frac{\partial D}{\partial t} \ \frac{\partial T}{\partial z} \bigg|_{-D} \tag{2.3}$$

$$\frac{\partial}{\partial t} \ T_{(z)} = \delta Re^{z} \tag{2.4}$$

Where δ is the extinction coefficient, .002 cm^{-1}, D is the mixed layer depth, R is the incident solar radiation in cal cm^{-2}sec^{-1}, (G-D') is the wind energy available for mixing, as defined by (G-D') = $m\bar{U}_{10}\tau_0(\rho_0 \propto g)^{-1}$. B is the back radiation from the sea surface, T_s is the sea surface temperature, and T_{-D} is the temperature below the thermocline. H is a step function defined by:

$$H \begin{cases} = 0 \text{ if } \dfrac{\partial D}{\partial t} \leq 0; \text{ no entrainment} \\[2mm] = 1 \text{ if } \dfrac{\partial D}{\partial t} > 0; \text{ entrainment at } z = -D \end{cases}$$

The value of H controls the mode of the equations. When H is zero, the equations are in a heat dominated mode, and a new thermocline will form at a depth shallower than the original thermocline, as in figure 2.1. H will equal zero when the combination of mixing energy and insolation is such that the old depth of the mixed layer cannot be maintained under current conditions. When H equals one, normal deepening of the mixed layer occurs, as forced by wind energy and controlled by the temperature gradient below the mixed layer.

3. Computational Scheme

The problem of putting these two sets of equations into an integrated model was substantial, because any inaccuracy in interfacing the two sections would cause large differences in the final solution.

The equations of motion (1.9 and 1.10) were used in a finite difference analog format, as was equation 2.2 for use in the computer.

To make the model as general as possible in a predictive mode, and to satisfy a Coast Guard operational constraint, a simple algorithm for the radiative boundary condition was used. I used a sine curve from 0 to π, with the zero point being 0600 local time, the maximum at $\pi/2$ at 1200 local, and π at 1800 local. From 1800 to 0600 the insolation R = 0. Back radiation was a constant.

To determine any deepening in the mixed layer, the value of $\partial D/\partial t$ was solved for in 2.2 by setting H = 1. If $\partial D/\partial t$ was greater than zero, showing the assumption of H = 1 to be correct, the system was shown to be in the wind driven mode, and the model progresses to the next time step. If $\partial D/\partial t$ was less than or equal to zero, the system entered the heat driven mode. By setting H = 0 in 2.2, and solving for (G-D');

$$(G-D') = \frac{1}{2} D[R(1+e^{-\delta D}) + B] - R\delta^{-1}(1-e^{-\delta D}) \tag{3.1}$$

This is similar to Denman's (21). D was solved for by Newton's technique. The difference in mixed layer temperature was found by integration of 2.1, substituting in 3.1, I obtain:

$$\Delta T_s = [R(1-e^{-\delta D}) + B] \ \Delta t/D \tag{3.2}$$

5

INITIALIZE BT PROFILE
WINDS, DISSIPATION COEFF
COMPUTE D   SET DNEW=0

INCREMENT TIME STEP
COMPUTE THERMAL
GRADIENT AT Z=DNEW

IF LAYER DEEPENS, SET AVERAGE
VELOCITIES FROM Z=0 TO Z=DNEW

D=DNEW

APPLY VELOCITY EQUATIONS AT ALL
DEPTHS THROUGH MIXED LAYER

COMPUTE RADIATIVE FLUX

COMPUTE DEEPENING BY 2.2

$\frac{\partial D}{\partial t} > 0$ NO   APPLY HEAT EQUATIONS
                                                3.1 TO DETERMINE DNEW

YES

COMPUTE ΔT_s
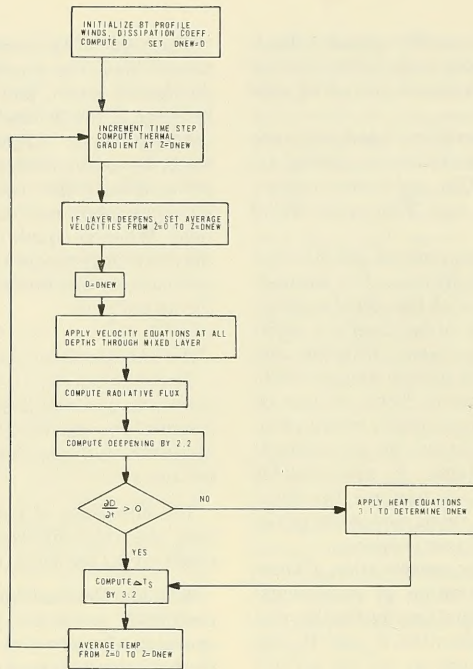BY 3.2

AVERAGE TEMP
FROM Z=0 TO Z=DNEW

Figure 3.1   Flowchart of the Model Computational Scheme.

T_s was solved for in all time steps, whether the mode of the model was heat or wind driven. Any penetration of solar radiation such that water below the mixed layer is warmed is accounted for by 2.4.

Because of the nature of the deepening cycles, and the possibility of the formation of a shallower mixed layer by heating (Figure 2.1), it becomes necessary to consider the effect of a layer of water near the surface, bounded by a temporary thermocline, deepening into a water layer already set into motion by a previous wind event. Since the entrained water already has momentum, some account of this momentum must be made. Since there is rapid mixing throughout the wind forced layer, this "entrained momentum" can be accounted for in a similar manner as was the temperature. Therefore, before each time step of current computations, an average velocity is taken over the entire deepened layer. (Pollard, Rhines and Thompson, 1973)

A time step of 900 seconds was used throughout the model to minimize the amount of error in the numerical solution and to more clearly differentiate the time where the Denman equations transfer from the wind forced to the heat driven modes. The entire computation scheme is illustrated in the flowchart of Figure 3.1.

Figure 3.2 shows a result of the model illustrating the possibility of velocity shears and changes in mixed layer thickness. This is a part of the run testing the mixed layer deepening section of the program. At time = 146 hours, three different velocity fields are seen. From the surface to 19.9 meters is seen the mixed layer and currents produced by the current wind event. The values at 20 meters are for a wind event earlier than the current one that produced mixed layers to a depth of 20 to 25 meters. A third wind event, the first chronologically, produced the strong, decaying velocities between 25 and 40 meters. This earliest wind event produced a mixed layer between 40 and 45 meters deep. One hour later, it is seen how the wind forced water entrains the fluid beneath it, while the lower layers continue unforced.

6

TIME:146.00 HOURS.   TAU   X: 0.00 TAU Y: 0.37 WIND DIR AND SPD: 0 550   MIXED LAYER DEPTH (CM): 1990 CLOCK HOUR: 17

TRANSPORT (M)

D	U	V	R	DIR	E	N	TEMP	DENSITY
0	4.38	0.50	4.41	83.5	16754	1541	8.36	1.02460
5	4.38	0.50	4.41	83.5	16752	1501	8.36	1.02460
10	4.38	0.50	4.41	83.5	16746	1433	8.36	1.02460
15	4.38	0.50	4.41	83.5	16442	1266	8.36	1.02460
20	0.04	0.85	0.85	2.4	14018	294	8.15	1.02466
25	4.96	0.05	4.96	89.4	11515	-719	7.89	1.02473
30	4.96	0.05	4.96	89.4	8460	-903	7.89	1.02473
35	4.96	0.05	4.96	89.4	5300	-112	7.89	1.02473
40	4.96	0.05	4.96	89.4	1107	326	7.89	1.02473
45	0.00	0.00	0.00	0.0	0	0	6.21	1.02534
50	0.00	0.00	0.00	0.0	0	0	6.17	1.02547

TIME: 147.00 HOURS.   TAU X: 0.00 TAU Y: 0.37 WIND DIR AND SPD: 0 550 MIXED LAYER DEPTH (CM): 2028 CLOCK HOUR: 18

TRANSPORT (M)

D	U	V	R	DIR	E	N	TEMP	DENSITY
0	4.18	-0.40	4.20	95.4	16902	1539	8.35	1.02460
5	4.18	-0.40	4.20	95.4	16905	1499	8.35	1.02460
10	4.18	-0.40	4.20	95.4	16899	1431	8.35	1.02460
15	4.18	-0.40	4.20	95.4	16595	1253	8.35	1.02460
20	4.18	-0.40	4.20	95.4	14133	297	8.35	1.02460
25	4.65	-1.75	4.96	110.6	11688	-758	7.89	1.02473
30	4.65	-1.75	4.96	110.6	8633	-942	7.89	1.02473
35	4.65	-1.75	4.96	110.6	5473	-151	7.89	1.02473
40	4.65	-1.75	4.96	110.6	1280	287	7.89	1.02473
45	0.00	0.00	0.00	0.0	0	0	6.21	1.02534
50	0.00	0.00	0.00	0.0	0	0	6.17	1.02547

Figure 3.2   Model output after a period of variable winds; D = depth in meters; U = northward velocity in cm/s; V = eastward velocity in cm/s; R = resultant velocity magnitude; DIR = resultant velocity direction.

7

TIME: 148.00 HOURS.   TAU X: 0.00 TAU Y: 0.37 WIND DIR AND SPD: 0   550 MIXED LAYER
DEPTH (CM): 2072   CLOCK HOUR: 19

TRANSPORT (M)

D	U	V	R	DIR	E	N	TEMP	DENSITY
0	3.87	-1.26	4.07	108.0	17051	1505	8.35	1.02460
5	3.87	-1.26	4.07	108.0	17049	1465	8.35	1.02460
10	3.87	-1.26	4.07	108.0	17048	1397	8.35	1.02460
15	3.87	-1.26	4.07	108.0	16739	1219	8.35	1.02460
20	3.87	-1.26	4.07	108.0	14277	263	8.35	1.02460
25	3.70	-3.31	4.96	131.9	11836	-857	7.85	1.02473
30	3.70	-3.31	4.96	131.9	8781	-1041	7.89	1.02473
35	3.70	-3.31	4.96	131.9	5621	-250	7.89	1.02473
40	3.70	-3.31	4.96	131.9	1428	188	7.89	1.02473
45	0.00	0.00	0.00	0.0	0	0	6.21	1.02534
50	0.00	0.00	0.00	0.0	0	0	6.17	1.02547

Figure 3.2   (*Continued*) Model output after a period of variable winds.

RESULTS

In testing the model, I used a two phase procedure, due to the unavailability of combined current and thermocline data. I first tested the mixed layer deepening portion, then the current portion. The combined result should be valid because of superposition. The basic assumptions of the two sections are comparable.

1. Variations in the Thermal Structure

I tested the equations dealing with the variations in the thermal structure against data taken at Ocean Station Papa, as presented by Denman and Miyake (1973). I ran my model for both the two day storm period of 21-23 June 1970 and the longer record of 13-20 June. Because of the generalized form of the radiative flux which I used, the agreement between the data and my model lacks during some days, but overall the fit is good. Figure 4.1 shows the values obtained for mixed layer deepening over the Gaussian-shaped storm of 21-23 June, and Figure 4.2 shows the fit of the sea surface temperature prediction for the same period.

Overall the fit between the curves is very good. The temperature curve shows a +0.1 degree C bias towards the end of the record. This is due to the fact that the actual value of the radiative flux was about one half of the average value I used in my computations. This caused the predicted temperature to be higher than the actual temperature due to the higher flow of heat into the model.

The coefficients I required for this fit were close to those found by Denman and Miyake (1973). The value I found for the amount of wind energy available for mixing as .0014, close to the Denman and Miyake value of .0012, and close to the value they calculated from Kato and Phillips (1969) of .0015. The value for the extinction coefficient was .002 cm^{-1}.

The other area of comparison was to the long data record of 13-20 June. (Figures 4.3, 4.4) I compared both the sea surface temperature and bathythermal profile during the entire period. Again, the overall fit is good. The areas of greatest departure on 16 and 17 June are due to the low actual values of the radiative input for those dates, causing the predicted temperature to become higher than the actual temperature for those dates. Late on 14 June (local), the marked difference in temperature is due to an abnormally high radiative flux late in the daylight hours of the 14th, which my generalized radiation format did not take into account. For an operational use, however, this generalized radiation boundary condition is necessary, because such data is not commonly available at sea.
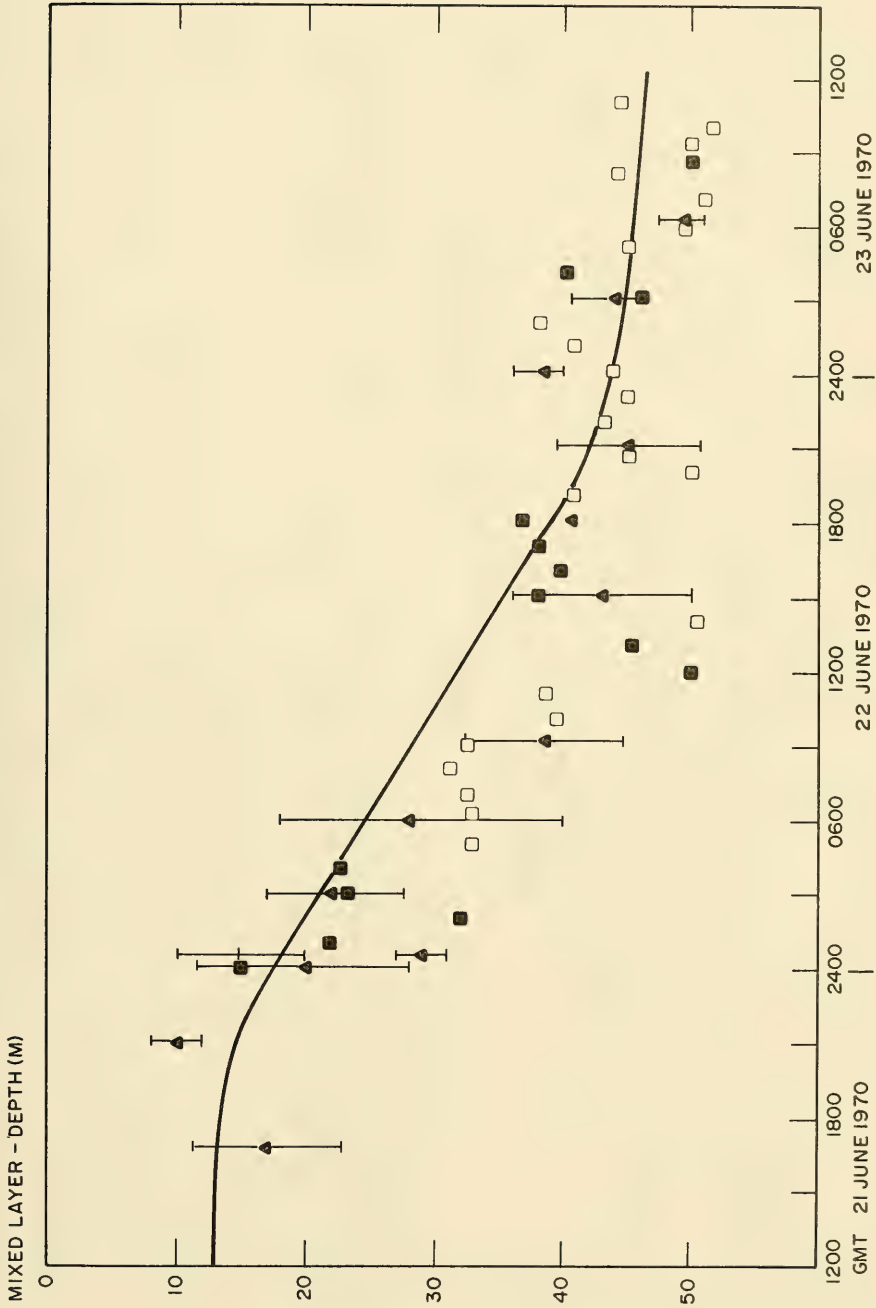
8

MIXED LAYER – DEPTH (M)

Figure 4.1   Deepening of the mixed layer during a Gaussian shaped storm.

9

Figure 4.2   Sea surface temperature change during Gaussian shaped storm.

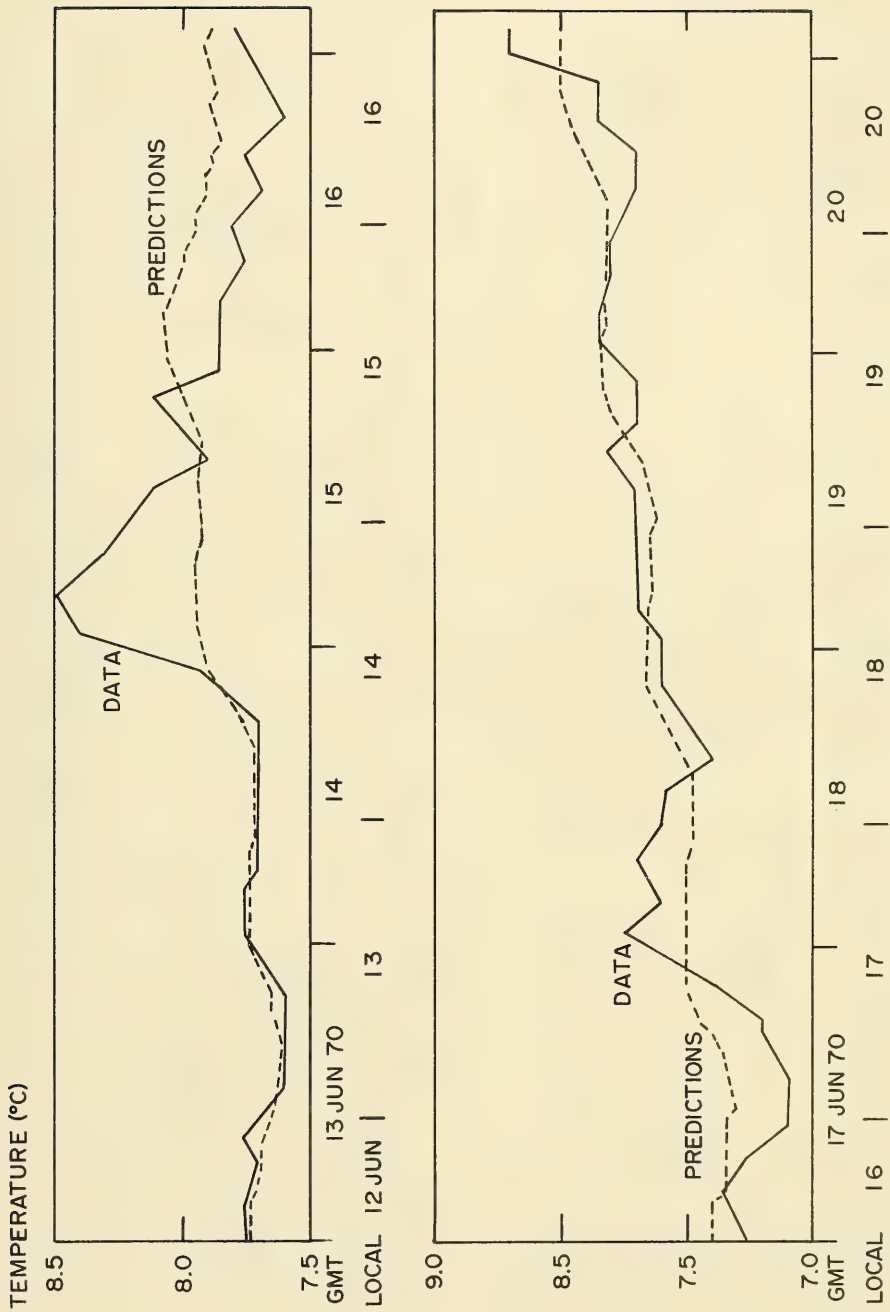10

TEMPERATURE (°C)

Figure 4.3   Sea surface temperature changes over 10 days of data
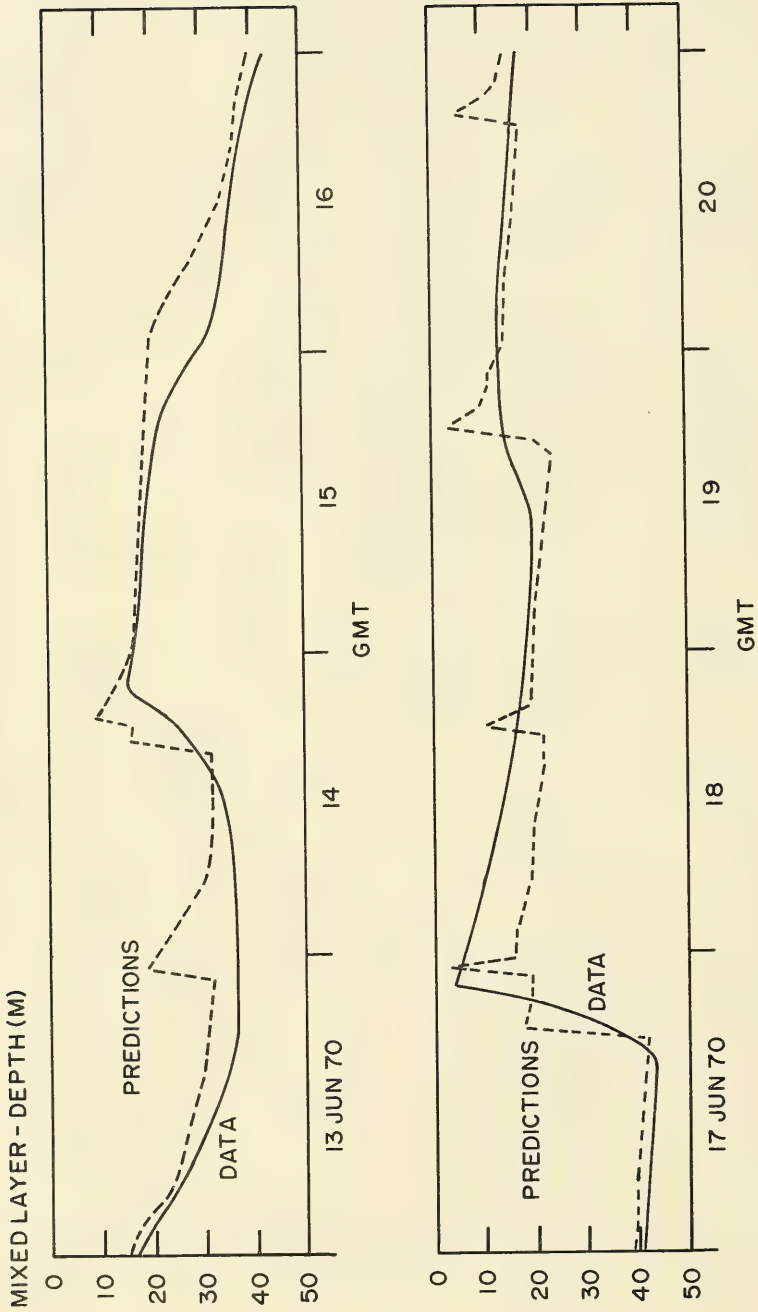
————— = Data

------ = Predictions

11

Figure 4.4 Deepening of the mixed layer with time
——— = Data
------ = Predictions

12

In an operational model, however, a factor for the cloudiness could be put in.

The visual quality of the fit in figures 4.3 and 4.4 is backed by statistical evidence. The average deviation of the prediction from the data in the sea surface temperature was slight. The prediction exceeded the data by 0.02°C on the average, but the hypothesis that the deviation between the two was zero was statistically significant in excess of the 75% level.

The average deviation of the prediction over the data is mixed layer depth was 1.04 meters, and here the results were significantly in excess of the 90% level.

2. Wind Driven currents in the mixed layer

The data used to test the current portion of the model was from Mooring 280 set by Woods Hole Oceanographic Institution in 1968. The mooring was set at 39-10 N, 70-03 W. The instruments provided wind data at 2 meters above the sea and current data at a depth of 12 meters for 48 days.

In using this data set, several problems were encountered. First, a sea current existed at the mooring throughout the record, tending approximately 045° - 065° magnetic, the velocity being about 20 cm sec^{-1}. Although there were strong inertial oscillations throughout the record, they were difficult to separate from the overall record because of the strength of the current and the noise in the data set. For these reasons, I was unable to separate clearly the inertial oscillations from the overall record using basic Fourier Analysis. I did not have at my disposal the complex filtering schemes which would have been necessary to separate out the oscillations. (Millard, 1978)

A more fundamental problem exists with the testing of a model of this sort with moored current data. My equations are Eulerian equations, because the assumption of the Rossby number being less than one eliminates the non-linear terms. In truth, however, the model is is Lagrangian. As the water particle moves, it is accelerated by various forces, and the water column in question is changed by wind energy and insolation. These charges are relative to the current position of the water, not on the original position of that water. The Eulerian equations can be applied in the manner I have because of the assumption of zonal wind stresses. The data set from a moored array is an Eulerian one, showing the changes in the water moving past a fixed point. What occurs at this fixed point is not necessarily dependent on the conditions that are experienced at the point of measurement. In other words, the advection terms in the equations of motion become important. The Eulerian data can give a good first approximation only of the water movement, since any strong constant current in the area renders my assumption of the Rossby number being less than one invalid. Moored arrays would be useful and valid, however, in an area where there is no constant current, with horizontally homogeneous water and zonal winds for some distance away from the mooring, such as if the mooring were placed in the center of a gyre.

Therefore, the fit obtained from this data is tenuous at best.

The only method I could use to extract some reasonable inertial transport from the data was to use a vector solution for the net sea current in the area and subtract that net current from the data set, thereby leaving the inertial component. The tidal oscillations in the area are almost zero.

To solve for this net current, I hindcasted what the frictionless inertial period transport would be, given the wind field in a certain data window under study. I then took the overall data and solved for the sea current. This frictionless solution may be used because we know that the ocean is close to being "frictionless." I used the following vector solution:
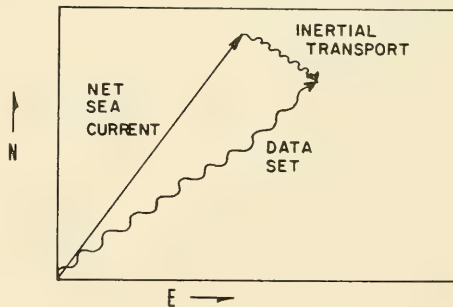

Figure 4.5 Lagrangian view of solution for Net Sea Current.

The "net sea current" as obtained above was subtracted from the data set to give the inertial transport. This "net sea current" as solved for above was not necessarily consistent over the

entire data window, however. The current patterns in the area were complicated by the mooring being on the northern fringe of the Gulf Stream. Changes in Gulf Stream flow caused consequent changes in the currents at the mooring. The currents were further changed in the second half of the record by a warm core ring which was located near the mooring from November 1 through 10.

Because of the procedure used to obtain the inertial oscillations, I tried to obtain dissipation coefficients which would provide an optimum fit for both the inertial transport solved for by the above method; and for best fit when adding the prediction and the computed net sea current and comparing these to the data set.

The method I used to test the model and adjust the K_1 and K_2 coefficients was basically trial and error, and judging the quality of fit from the length of the vectors connecting points of equal time in both sets. One result I discovered while testing the model was that the K_1, or second order dissipation term controlled the velocity of the model, and the K_2, or first order dissipation term controlled the angle the current made with the wind, although each term had an effect on the other's domain. This result may be an artifact of the numerical method, or could be an indicator of part of the physical system.

The data used to fit the coefficients was three portions of the mooring 280 record. I chose these windows to correspond with certain characteristics of the wind record. Window I was a period of relatively constant winds from generally the same direction, from 26 October to 2 November. Window II examined constant velocity winds and varying direction. The winds varied 700 degrees in direction between 3 and 12 October. During Window III from 3 to 13 November, the winds varied both in speed and direction greatly.

One fundamental principle used to test the computer runs aginst the data must be pointed out. Because of the low amount of dissipation in the wind driven system, the old current motions present in the mixed layer will greatly affect the currents after the start of some new wind event. The results of an applied wind stress will vary greatly depending on the character of the velocity in the mixed layer before the start of that wind event. If the wind comes over an ocean at rest, the velocity and direction of flow will be very different than if similar conditions acted on a water mass already in motion. For these reasons, the wind history must be applied for some time previous to the start of the comparison with the current data. That time is taken to be four days, as after that time, the results of the initial value problem have been buried in the effects of the later wind history (Pollard and Millard, 1970). The verification of this principle can be seen in later presentations of my data.

The value for the radiative flux at the mooring location was extrapolated from the data of Hanson (1976). I calculated a radiation flux at $39°$ $10'N$, the latitude of the mooring, of 101.8 cal $cm^{-2} day^{-1}$. This value is the average for the value for October and November.

I will consider the results from each window separately. Data Window I covered the period of 26 October to 2 November. The winds throughout the period were blowing towards $110° \pm 30°$ Magnetic, with a velocity of 12-17 meters sec^{-1}. The current record shows strong inertial oscillations throughout. Figure 4.6 shows a Lagrangian view of the water trajectory over the entire data window, the water movement being the jagged line. The smoother line is the predictions. The straight lines connecting the two plots show the distance between the prediction and the data every 10 hours. Here the inertial oscillations in the prediction are effectively buried by the addition of the sea current.

Figure 4.7 shows this same data window, but with the inertial transport separated from the mean flow as described above. Figure 4.7 shows the prediction compared to the inertial period oscillations over the entire length of the data window. Figure 4.8 shows the last four days of the data and prediction. When comparing Fig. 4.7 and Fig. 4.8, it is easily seen how the delay in comparing the prediction to the actual current is necessary to eliminate old motions in the mixed layer, as the comparison between the prediction and the current is much closer after that time. The pronounced change in the direction of the data attests to this.

The 4 day lag hypothesis is also supported by statistical evidence. The hypothesis under study was that the deviation to the left of recombined net sea current and inertial currents was equal to the deviation of the prediction to the right of the separated inertial data. For the runs of the model compared to date after 0 days, such as figures 4.6 and 4.7, the hypothesis fails at all significance levels. When the companion is made after 4 days, however, the hypothesis passes at the 85% significance level.

START OF PLOT IS 0 DAYS
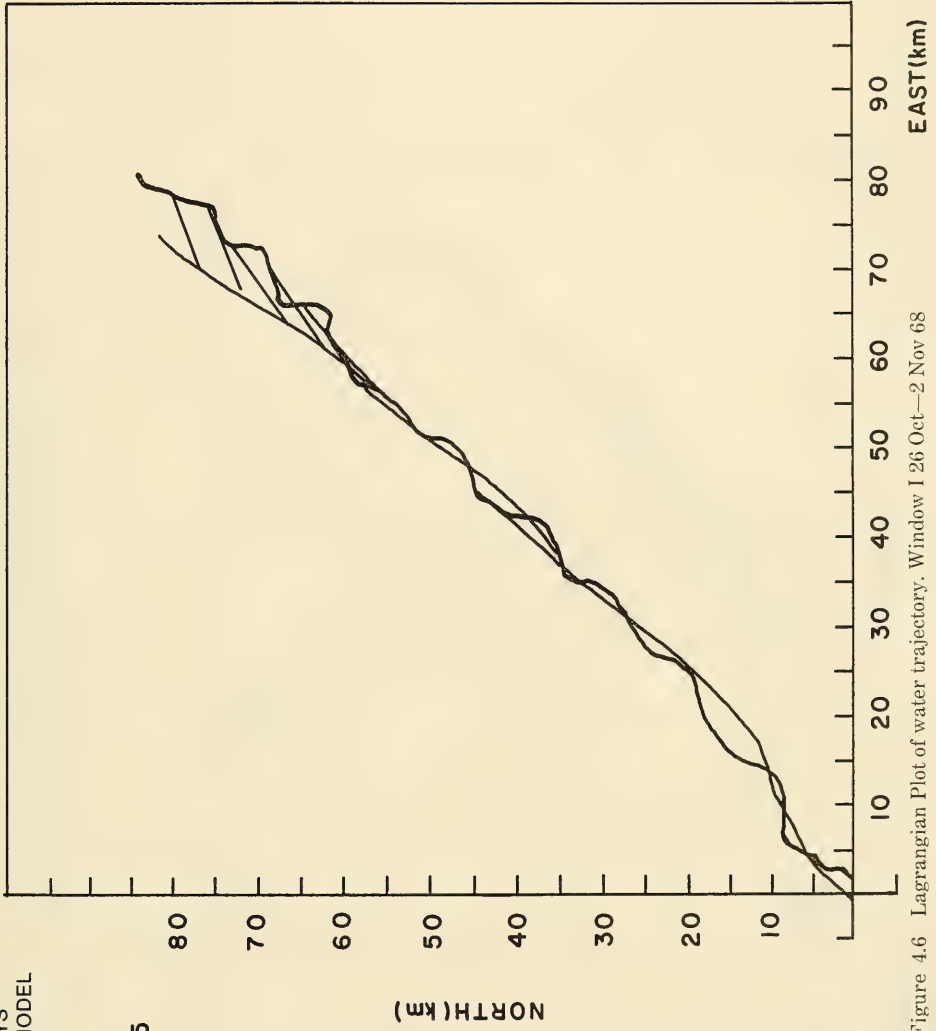AFTER START OF THE MODEL

4.1.5

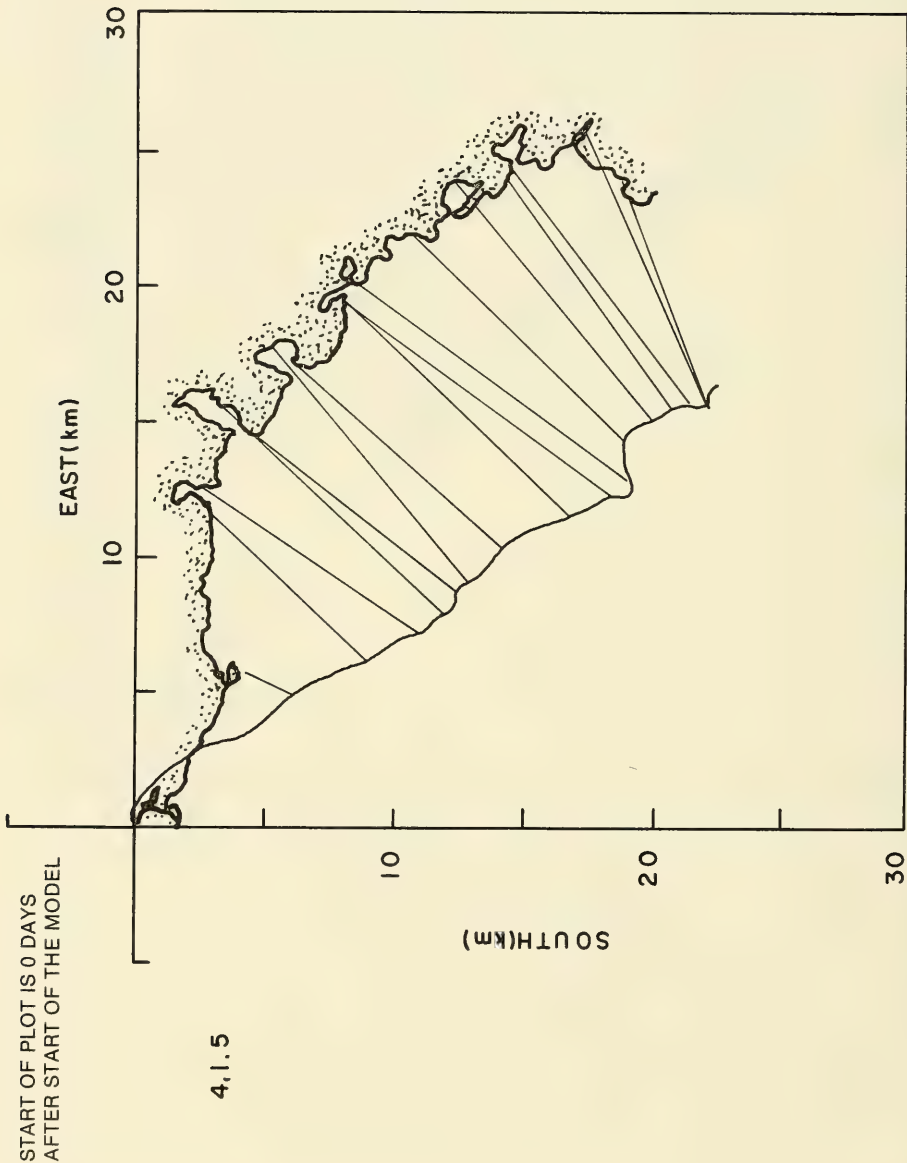Figure 4.6   Lagrangian Plot of water trajectory. Window I 26 Oct—2 Nov 68

15

START OF PLOT IS 0 DAYS
AFTER START OF THE MODEL

4.1.5

EAST(km)

SOUTH(km)

Figure 4.7 Inertial Period component of water trajectory Window I 26 Oct—2 Nov 68
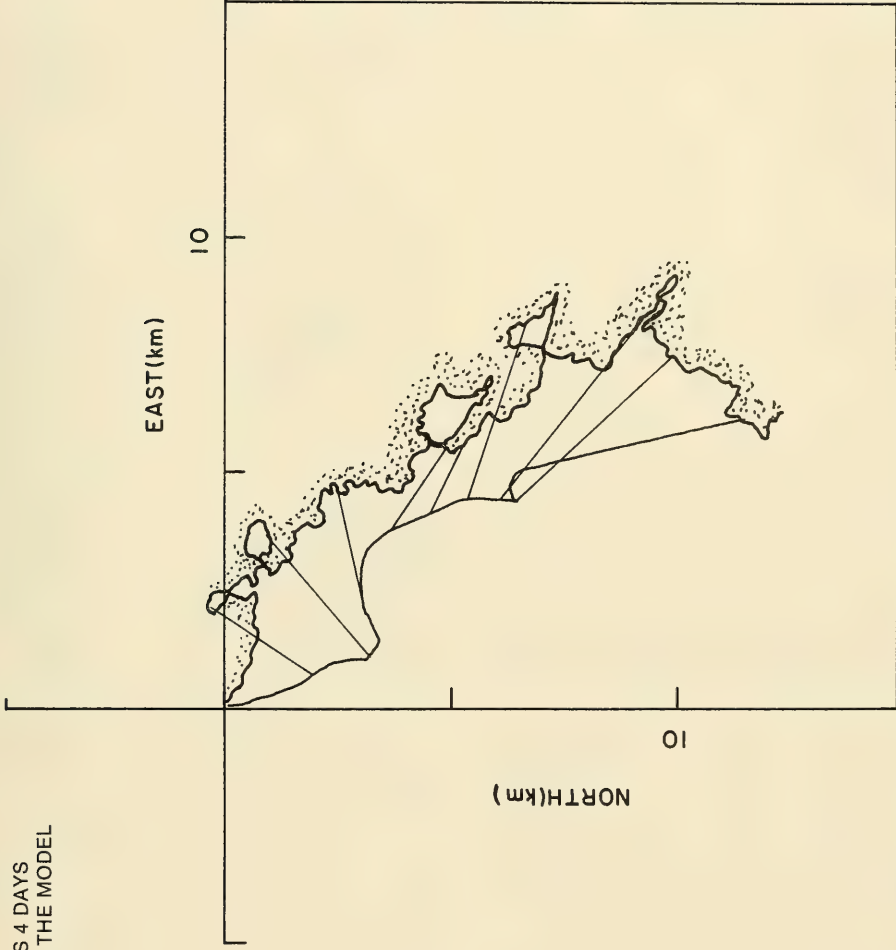
START OF PLOT IS 4 DAYS
AFTER START OF THE MODEL

4.1.5

EAST(km)

10

NORTH(km)

10

Figure 4.8 Inertial period component of water trajectory Window I 26 Oct—2 Nov 68

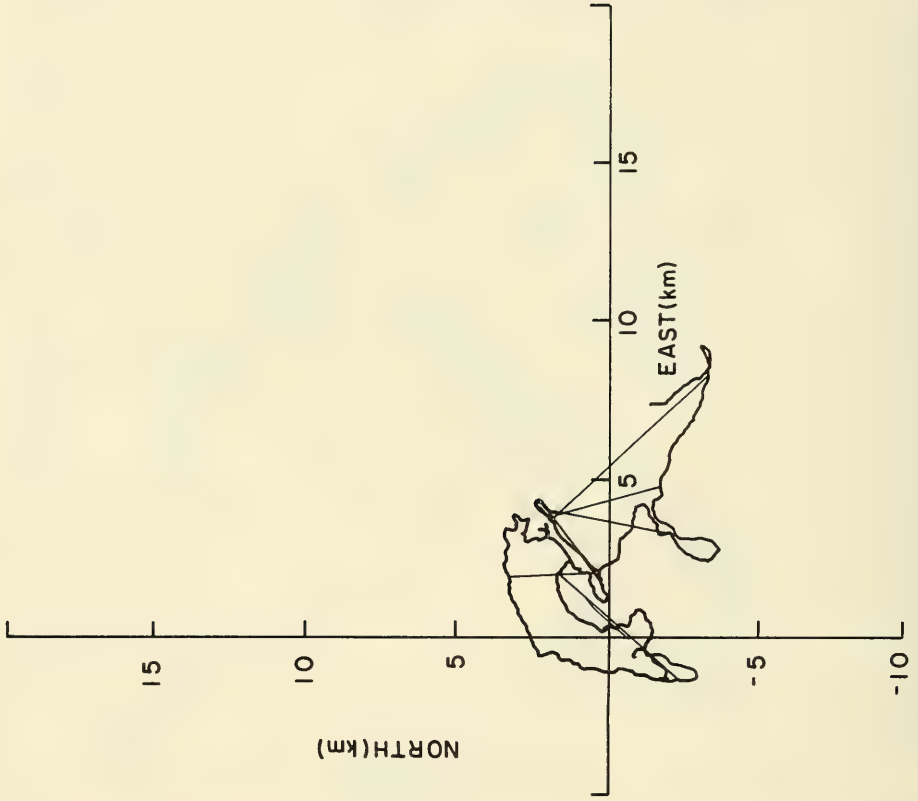17

START OF PLOT IS 4 DAYS
AFTER START OF THE MODEL

4.2.2

NORTH(km)

EAST(km)

Figure 4.9   Inertial period component of water trajectory Window II 3—12 October

18

In deriving the coefficients of dissipation, I tried to balance the fit obtained by looking at strictly the inertial transports versus the prediction and the fit obtained when recombining the prediction and the net sea current. For this reason, the plot of predictions is slightly to the right of the inertial period data, while the prediction recombined with the net sea current is slightly to the left of the data. The runs illustrated here provided the best fit overall. The coefficients required for this fit are:

$K_1 = 1 \times 10^{-7}$; second order dissipation term
$K_2 = 5 \times 10^{-5}$; first order dissipation term

Runs from data Windows II and III did not provide as useable testing values as Window I. Due to the variable nature of the winds, there was little overall transport, as shown in Figure 4.9. Figure 4.9 begins after 4 days have passed. Data Window II was used for this run. Both plots show the inertial period component of the Lagrangian particle trajectory.

The initial bathythermal profiles for all the runs illustrated above were taken at Ocean Weather Station Hotel near the dates in question. OWS Hotel was "upstream" of the mooring, so the profiles experienced at Hotel would be advected onto the mooring. Because of the lag involved between the measurements at Hotel and the mooring, I used BT traces preceding the time of the start of the model by one week to initialize the program.

Figure 4.11 shows the total data set. All the curves shown on the graphs are the data from the mooring. I was unable to superimpose on this plot the predictions of the model, unfortunately, due to time constraints. It is easily seen that large inertial oscillations occurred throughout the data record, and that a sea current towards the northeast existed throughout the record.

One could try to postulate what the mean current would be in the area by trying to set the mean velocity to zero within a certain window, but this would ignore currents that may be produced by steady winds, which are an important part of the testing of this type of model. Complex Fourier analysis would also be an answer, but it still would not answer the problems I showed earlier with Lagrangian vs. Eulerian conflicts and the testing of the velocity shears that have been shown to exist.

EXPERIMENTAL DESIGN

The problems I experienced with testing the model have prompted me to formulate an experimental design proposing a method to test an integrated model of this sort. To eliminate problems with the isolation of inertial frequencies from the constant current, the data should be taken in an area with a very low overall sea current, or no current at all. The area should have steady winds at most times to get a consistent transport for ease of testing. The mixed layer that is predominant in the area should be less than 100 meters deep, so that the velocities produced by the wind forcing are of a measurable and distinct character.

Simultaneous with the current measurements, the bathythermal profiles should be measured in both surface layers and below the thermocline, to determine surface warming and the temperature gradient at the thermocline. A pyroheliometer and some instrument measuring back radiation should also be included.

The most fundamental problem in the experimental design is the problem of Lagrangian vs. Eulerian measurement. Lagrangian is most desireable, but problems occur with measurement of currents at different depths. Accuracy in measurement must be = 1 km, so that the inertial oscillations can be accurately mapped. Drift buoys with drogues lack this accuracy, if satellite tracking were used. Satellite tracking also has the disadvantage that data points are much too far separated in time to be valid in inertial frequencies. The buoys could be followed with a ship, but the cost for such an operation would probably be prohibitive. Sofar floats could not be used due to the constantly changing density structure of the mixed layer. Therefore, we come back to an Eulerian measurement of a mooring. Eulerian data could be used reasonably, as long as one can assume horizontal homogeneity of the boundary conditions . . . insolation, winds, and bathythermal structure. The extent of the homogeneity must be greater than the total possible inertial transport over the length of the data record. If we assume an average inertial velocity of 5 cm sec^{-1}, the total transport over a 48 day data record would be 207 km.

I feel that the center of a gyre would provide all the factors I have outlined as necessary. The water conditions here are homogeneous over the extent of the gyre center. The North Atlantic
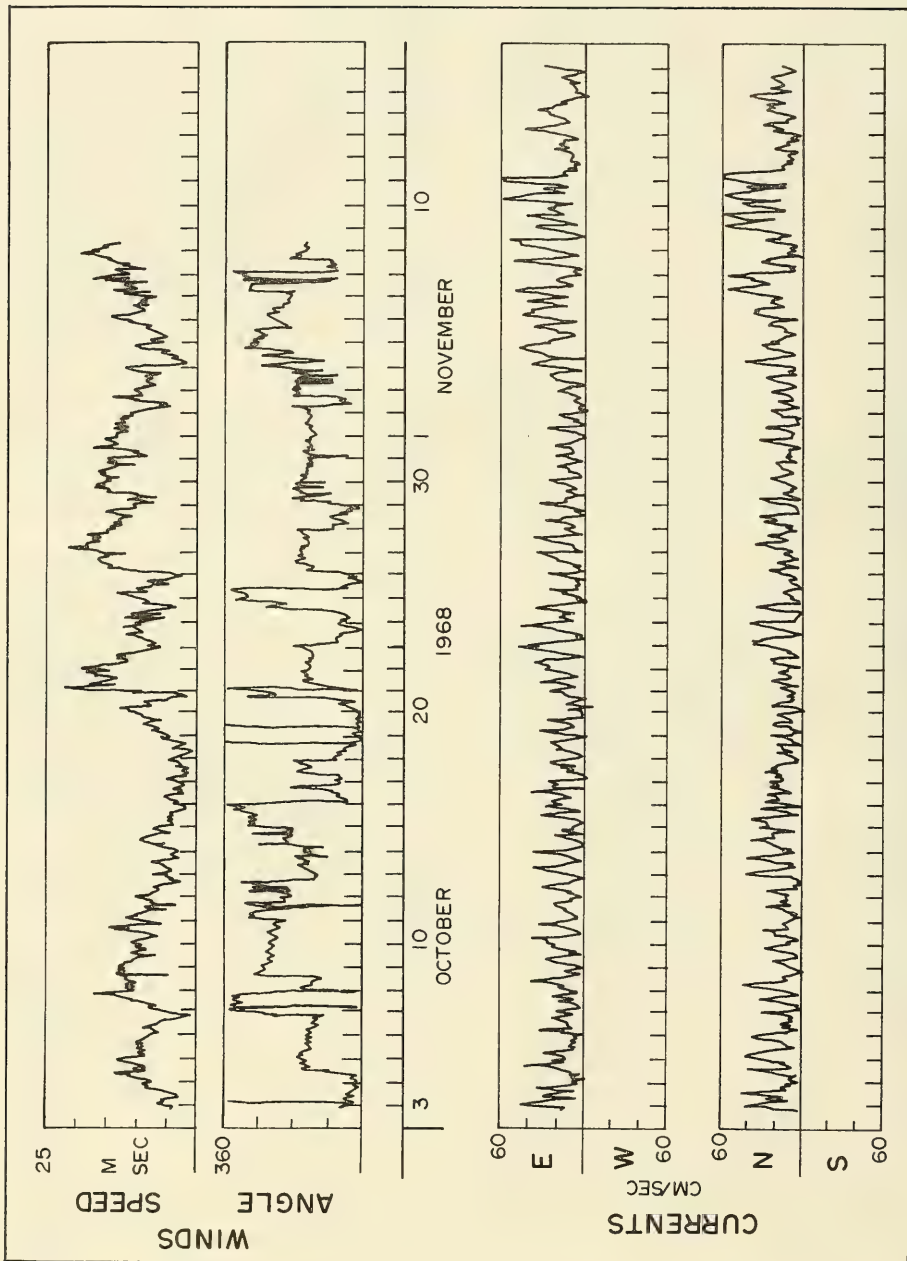
Figure 4.11   One Hour averages of winds and currents, Mooring 280

Gyre (32.5 N, 57.5 W) in May and June would be a suitable location. Here the sea currents average .45 k (23 cm sec^{-1}) with no consistent direction in a 5° square centered at the above position. A large portion of the currents in the region may be due to wind driven oscillations, due to the steady winds and shallow thermocline, as we shall see. The inertial frequency at this latitude is 22.33 hours. This should be separable from diurnal tidal oscillations, with a frequency of 24.8 hours. There exists a very shallow thermocline beginning near the surface of .06°C meter^{-1}. The thermal structure of the area is homogeneous for a radius of 500 km around the site. (U.S. Naval Oceano. Off. Pub. 700). Surface winds for May and June are mostly from S to SW, with a mean velocity of 12 knots with 16% of winds being 16-21 knots (Navaer 50-1C-528).

These shallow mixed layers and moderate winds should produce very strong intertial oscillations. Significant changes should also occur to the thermocline during this period due to the seasonal warming of the sea at this position, large wind stresses and shallow initial mixed layers.

The mooring itself should have current meters and thermistors spaced as closely as possible through the mixed layer and through the thermocline to record variations of the currents with depth in the mixed layer. The wind recorder should be mounted as high above the sea surface as possible, to free the wind measurements from near boundary processes as much as possible.

To determine more accurately the sea currents in the area, standard sections should be taken around the mooring when it is set and when it is retrieved to determine by dynamic methods the steady sea currents in the area.

CONCLUSIONS

I have, with reasonable success, modeled the wind driven inertial oscillations in the deep oceans, and demonstrated the importance of a two dimensional model on the solution for surface transport. This integration of thermocline models into the current models is very necessary because of the large effects of vertical structure on the total result. It is unfortunate that data in the two dimensions is not available, but the experiment I have proposed should yield data usable to test this type of model. Even with the data now available, more work can be done to obtain a better fit. Unfortunately, time constraints have forced me to stop work on testing the model at this point. The dissipation coefficients I found may well be much too high, for the modeled motions tend to die out much faster than the data as seen in Figure 4.11. More experience with statistical methods and demodulation of the data set to derive inertial motions would also be helpful. Hopefully this paper will stimulate more interest in the mixed layer and its atmospheric interactions.

REFERENCES

Assaf, G., R. Gerard and A. F. Gordon, 1979: "Some Mechanisms of Oceanic Mixing Revealed in Aerial Photographs." *J. Geophys. Res.*, 76,6550-6572.

Bodine, B. R., 1971: "Storm Surge on the Open Coast. Fundamentals of Simplified Predictions." *Tech. Memo. No. 35* U. S. Army Corps of Engineers Research Center, Maryland.

Defant, Albert, 1961: *Physical Oceanography.* New York, Pergamon.

Denman, K. L. 1973: "A Time Dependent Model of the Upper Ocean." *J. Phys. Oceano.* 3, 173-184.

Denman, K. L. and M. Miyake, 1973: "Upper Layer Modification at Ocean Station 'Papa': Observations and Simulation." *J. Phys. Oceanogr.*, 3, 185-196.

Ekman, V. W., 1905: "On the Influence of the Earth's Rotation on Ocean Currents." *Ark. Mat. Astron. Fys.*, 2, No. 11.

Gulf Stream Monthly Summary: U. S. Naval Oceanographic Office. 3, No. 10-11.

Hanson, Kirby J. 1976: "A New Estimate of Solar Irradiance at the Earth's Surface on Zonal and Global Scales." *J. Geophys. Res.*, 81, 4435-4443.

Kato, H. and O. M. Phillips, 1969: "On the Penetration of a Turbulent Layer into a Stratified Fluid." *J. Fluid Mech.*, 37, 643-655.

Kollmeyer, R. C. 1978: Unpublished Manuscript.

Kraus, E. B. ed. 1977: *Modelling and Prediction of the Upper Layers of the Ocean.* New York, Pergamon.

Marine Climatic Atlas of the World Vol I: North Atlantic Ocean (Navaer 50-1C-528). Washington, D.C.: U. S. Government Printing Office, 1955.

Millard, R. C. Jr., 1978: Personal Communication.

Mooney, K. A., 1977: *A Method for Manually Calculating the Local Wind Current*. Unpublished Manuscript.

Neumann, Gerhard and Willard J. Pierson, Jr. 1966: *Principles of Physical Oceanography*. Englewood Cliffs, N.J.: Prentice Hall, Inc.

Niiler, Pearn P. 1977: "One Dimensional Models of the Seasonal Thermocline. from *The Seas*, Vol. 6. New York, Wiley. 97-1115.

Oceanographic Atlas of the North Atlantic—Section I Physical Properties US Naval Oceanographic Office. 1967.

Pollard, R. T., 1970: "On the Generation by Winds of Inertial Waves in the Ocean." *Deep Sea Res.*, 17, 795-812.

Pollard, R. T. and R. C. Millard, Jr., 1970: "Comparison Between Observed and Simulated Wind Generated Inertial Oscillations." *Deep Sea Res.*, 17, 813-821.

Pollard, R. T., P. B. Rhines, and R.O.R.Y. Thompson, 1973: "The Deepening of the Wind Mixed Layer." *Geophys Fl. Dyn.*, 3, 381-404.

Richman, J. and C. Garrett, 1977: "The Transfer of Energy and Momentum by the Wind to the Surface Mixed Layer." *J. Phys. Oceano.*, 7, 876-881.

Smith, S. D. and E. G. Banke, 1974: "Variation of the Sea Surface Drag Coefficient with Wind Speed." *Quart J. Roy. Metero. Soc.*, 101, 665-673.